CESARE'22
3rd Coordinating Engineering for Sustainability And Resilience
May 6th – May 9th, 2022, Irbid, Jordan
ISSN:2788-6204

ESTIMATION OF FRICTION CAPACITY OF DRIVEN PILES IN SAND: EFFECT OF SAND DILATION

Ahmed S. Alawneh [1,*], Osama K. Nusier [1], Bayan N. Jaraha [2] and Nikos D. Lagaros [3]

[1] Department of Civil Engineering, Jordan University of Science &Technology, Irbid 2210, Jordan; nosama@just.edu.jo

[2] Graduate Research Assistant, Department of Civil Engineering, Jordan University of Science &Technology, Irbid 2210, Jordan; bnaljararha16@eng.just.edu.jo

[3] School of Structural Engineering, National Technical University of Athens (NTUA), 15780 Zografou, Greece; nlagaros@central.ntua.gr

* Corresponding Author: asshlash@just.edu.jo

Keywords: Friction, Driven Piles, Estimation, Dilation, Sand.

ABSTRACT

This paper is dedicated to investigate the effect of sand dilation during pile axial loading on ultimate shaft capacity of driven piles in sand based on a database comprising of 37 well-documented full-scale pullout pile load tests collected from literatures. The results indicated that the contribution of sand dilation during pile axial loading to the measured shaft capacity is significant for piles with diameter less than 0.40m in medium dense and dense sand especially at low stress level. In some cases, sand dilation may contribute to as high as 45% of the measured shaft capacity. For piles with diameter greater than 0.60m, the contribution of sand dilation to the measured shaft capacity is small and generally less than 10% especially at high stress level. A design methodology for tension piles in sand which incorporates the effect of sand dilation is proposed in this study. The validity of the proposed method was verified by comparing prediction with measurement made on a well-documented field case from literature. The comparison indicated that the proposed approach gives reasonable prediction and thus can be used to predict shaft capacity of driven piles in sand.

1. INTRODUCTION

Driven piles are generally used to support structures such as highway bridges, towers and offshore structures such as floating and fixed platforms. The load transfer mechanism in piles is through shaft friction and end bearing pressure. Even though recent studies (Chow 1997, Jardine et. al. 2005, Lehane et. al 2005) led to new design methods for driven piles in sand, estimation of shaft friction component of driven pile capacity in sand still involve some level of uncertainty due to involvement of many influencing factors. These factors include soil properties, pile characteristics, friction fatigue processes during pile driving, time effects (pile set-up), pile-sand interface friction angle, changes in radial effective stress during pile axial loading (effect of sand dilation) and effect of cyclic loading (Chow et. al 1998, Alawneh et al. 1999, Randolph et. al 1994, Jardine et. al. 2005, Lehane et. al 2005, Igo et al. 2011). Unfortunately, none of the current design methods considered all these factors when assessing shaft or end bearing capacity of driven piles in sand. Moreover, some of the current design methods are not consistent with observed pile behavior during pile installation and axial loading.

The ultimate shaft capacity of a driven pile in sand of outer diameter = D and penetration depth = L is usually determined using the following equation:

ISSN:2788-6204

$$Q_s = \pi\, D \int_0^L \tau_f \; dz \qquad (1-a)$$

$$\tau_f = \sigma'_{rf}\, tan\delta_f \qquad (1-b)$$

Where Q_s= shaft friction capacity, z = depth below ground surface, τ_f = local unit shaft friction at failure, σ'_{rf}= radial effective stress at failure acting on pile surface and δ_f = pile-sand friction angle at failure. During pile driving, the sand in front of the pile tip moves in the vertical as well as in the radial directions leading to densification of the sand mass around the pile. By the time the pile reaches its final penetration, the radial effective stress acting on the pile shaft is generally greater than the initial at-rest value before pile driving. At any depth, the radial effective stress acting on pile surface after driving and before uplift loading is termed stationary radial effective stress, σ'_{rc}. Changes in radial effective stress on pile surface occur not only during pile driving but also during pile axial loading due to the tendency of the sand to dilate at the pile-sand interface. Sand dilation at the interface is not free to occur since the surrounding sand mass acts on the interface by its lateral stiffness. This leads to a change (increase) in the magnitude of the radial effective stress by a value equal to $\Delta\sigma'_{rd}$. As such, the radial effective stress at failure, σ'_{rf}, is the sum of two components; the stationary and the dilation components:

$$\sigma'_{rf} = \sigma'_{rc} + \Delta\sigma'_{rd} \qquad (1-c)$$

Substitute Eq. (1-c) into Eq. (1-b) to get:

$$Q_s = \pi\, D \int_0^L (\sigma'_{rc} + \Delta\sigma'_{rd})\, tan\delta_f \; dz \qquad (1-d)$$

Or, the ultimate shaft friction capacity can be written as the sum of two components; the contribution of the stationary radial effective stress to shaft capacity (Q_{sc}) and the contribution of the change (increase) in radial effective stress during pile axial loading to shaft friction capacity (effect of sand dilation), ΔQ_{sd}:

$$Q_s = Q_{sc} + \Delta Q_{sd} \qquad (1-e)$$

$$Q_{sc} = \pi\, D \int_0^L (\sigma'_{rc}\, tan\delta_f)\, dz \qquad (1-f)$$

$$\Delta Q_{sd} = \pi\, D \int_0^L (\Delta\sigma'_{rd}\, tan\delta_f)\, dz \qquad (1-g)$$

This paper is devoted to investigate the relative contribution of the change in radial effective stress (effect of sand dilation) to shaft capacity of driven piles in sand. A database comprising of 37 full-scale pile load tests collected from literature are analyzed and simplified correlations are proposed to estimate pile shaft capacity as the sum of two components; the contribution of the stationary radial effective stress and the change in radial effective stress during pile axial loading (effect of sand dilation).

2. Database

The database of this study consists of 37- full-scale pull out pile load tests collected from literature (12 closed-ended steel pipe piles and 13 open-ended steel pipe pile, 10 closed-ended concrete piles, 1 open-ended concrete pile and 1 timber pile). Pile characteristics, soil properties and load measurements for the closed and open-ended piles are summarized in Tables (1) and (2), respectively.

ISSN:2788-6204

Table 1: Pile characteristics, soil properties and load measurements for the closed-ended piles

Site Name (Reference)	Site No.	Serial No.	Pile No.	L (m)	D (m)	Pile type	γ'_{ave} (kN/m^3)	σ'_{tip} (kN/m^2	$\sigma'_{v,ave}$ (kN/m^2)	φ_{cv} (°)	φ (°)	D_r (%)	Meas. Q_s (kN)
Low Sill Structure, Old River, Louisiana (Mansur et al., 1958)	1	1	2	19.81	0.56	Steel	8.10	160.5	80.3	30	34	65	1680
		2	4	20.12	0.46	Steel	8.10	163.0	81.5	30	34	62	1780
		3	5	13.72	0.46	Steel	7.90	108.4	54.2	27	30	57	715
		4	6	19.81	0.51	Steel	8.00	158.4	79.2	30	34	55	1655
Arkansas River Lock and Dam No. 2 (Sherman et al., 1974)	2	5	G-2	13.04	0.35	Conc.	15.90	174.0	87.0	30	36	70	803*
		6	B-5	13.10	0.46	Conc.	13.34	140.6	70.3	30	36	70	1005*
Arkansas River Lock and Dam No. 3 (Sherman et al. 1974)	3	7	G-7	11.67	0.33	Timber	13.18	153.8	76.9	30	34	55	433
Arkansas River Lock and Dam No. 4 (Mansur and Hunter, 1970)	4	8	1	16.18	0.38	Steel	10.29	166.5	83.3	30	34	63	828
		9	2	16.08	0.51	Steel	10.29	165.4	82.7	30	34	63	1000
		10	3	16.15	0.56	Steel	10.30	166.4	83.2	30	34	63	1080
		11	4	12.28	0.41	Conc.	10.30	126.5	63.2	30	34	63	820
		12	10	16.18	0.51	Steel	10.30	166.7	83.3	30	34	63	980
Jonesville Lock and Dam (Sherman et al., 1974)	5	13	1	11.58	0.46	Conc.	12.33	142.80	71.4	32	37	70	1128
		14	2	13.72	0.46	Conc.	11.94	163.8	81.9	32	37	70	1300
		15	3	16.42	0.46	Conc.	11.67	191.6	95.8	32	37	70	1116
		16	4	13.72	0.46	Conc.	11.94	163.8	81.9	32	37	70	1123
Ogeechee Georgia (Vesic, 1970)	6	17	H16	15.00	0.46	Steel	11.84	177.6	88.8	31	40	73	1540
Dramman Norway (Gregersen et al., 1973)	7	18	A	8.00	0.28	Conc.	11.25	90.0	45.0	30	31	25	94
		19	D/A	16.00	0.28	Conc.	11.09	177.4	88.7	30	31	25	254
		20	E	23.50	0.28	Conc.	10.70	251.4	125.7	30	31	25	287
Hoogzands, the Netherland (Beringen et al., 1979)	8	21	II	6.75	0.36	Steel	16.00	108.0	54.0	33	42	90	1106
Labenne Site (Lehane et al., 1993)	9	22	TP2	5.95	0.10	Steel	13.10	78.0	39.0	33	34	45	50
Hsina-Ta (Yen et al., 1989)	10	23	5	34.30	0.61	Steel	9.06	310.6	155.3	30	33	50	2500

*Excluding clay layer.

ISSN:2788-6204

Table 2: Pile characteristics, load measurements and soil properties for the open-ended piles

Site Name (References)	Site No.	Serial No.	Pile No.	L (m)	D (m)	Pile type	γ'_{ave} (kN/m^3)	$\sigma'_{v,tip}$ (kN/m^2)	$\sigma'_{v,ave}$ (kN/m^2)	φ_{cv} (°)	φ (°)	Dr (%)	Meas. Q_s (kN)
Hoogzand Holland (Beringen et al., 1979)	8	1	I	7.00	0.36	Steel	15.71	110.0	55	33	43	90	817
		2	III	5.25	0.36	Steel	16.38	86.0	43	33	43	90	538
Padre Island (McClelland Engineers Inc. 1958)	11	3	A	14.83	0.51	Steel	10.45	155.0	77.5	30	34	59	481
British Columbia (McCammon and Golder, 1970)	12	4	IA	45.42	0.61	Steel	7.85	356.6	178.3	30	32	35	1637
North Sea (AD) (Fugro, 1969)	13	5	P16	30.50	0.61	Steel	9.40	286.8	143.4	30	34	60	2531
Blount Island (Nottingham, 1975)	14	6	322	22.56	0.27	Steel	8.48	191.2	95.6	30	34	59	702
Mustang Island (Reese and Cox, 1976)	16	7	1	21.03	0.61	Steel	9.04	190.2	95.1	33	38	82	1823*
		8	2	21.03	0.61	Steel	9.04	190.2	95.1	33	38	82	1677*
Dunkerque (Brucy et al., 1991)	17	9	CS	11.60	0.32	Steel	12.16	141.0	70.5	30	34	60	388
Los Barrios (Mey et al., 1985)	18	10	1	18.00	0.91	Conc.	10.00	180.0	90.0	30	33	50	2500
Dunkirk (Jardine and Standing, 2000)	19	11	R1	19.30	0.48	Steel	10.88	210.0	105.0	32	36	78	1450
Euripides (Kolk et al., 2005)	20	12	Ia	30.50	0.76	Steel	10.49	320	160.0	33	43	85	3000*
		13	Ib	38.70	0.76	Steel	10.41	403	201.5	33	42	90	9750*
		14	II	46.70	0.76	Steel	10.21	477	238.5	33	42	90	11000*

*Excluding clay layers.

Pile characteristics include pile length, pile diameter, pile type (concrete, steel, timber), and pile end type (closed or open-ended pile). Soil properties, which are taken from the quoted references, include average unit weight, average effective vertical stress, friction angle and relative density of sand. In Tables (1) and (2), the measured uplift loads, Q_s, are those cited in the quoted references.

2.1 Increase in Shaft Capacity during Pile Axial Loading (Effect of Sand Dilation)

The mechanism of shaft friction mobilization along the pile shaft can be simulated by a simple model test called "Interface Direct Shear Test" with a prescribed normal stiffness constant (k). A steel plate is placed in the bottom half

ISSN:2788-6204

of the shear box with roughness equal to that for the shaft material. The soil specimen is placed in the upper half of the shear box as illustrated in Figure (1). During shear process, the steel plate slides against the soil specimen which is subjected to an initial normal stress. During shear loading, the soil tends to dilate and the normal effective stress increases. During pile axial loading, the soil at the interface tends to dilate and at the same time the surrounding soil mass acts on the interface by its lateral stiffness. The lateral stiffness of the surrounding soil mass is represented by an elastic spring with stiffness constant equals to (k) which generates an increase in the magnitude of radial effective stress at ultimate loading equal to $\Delta\sigma'_{rd}$. Figure (2) represents a schematic representation of pile-soil interface behavior during axial loading.

Based on the cavity expansion theory in an infinite soil mass, the increase in the radial effective stress due to pile-sand interface dilation, $\Delta\sigma'_{rd}$, can be calculated from the following equation (Lehane and Jardine, 1994):

$$\Delta\sigma'_{rd} = \frac{4\, G_{\circ}\, \delta_h}{D} \qquad (2-a)$$

Where $G_{\circ}$= small strain shear modulus of sand and δ_h= radial displacement of the pile-sand interface at ultimate loading (dilation). Based on small-scale instrumented model pile tests, Chow (1997) proposed to use δ_h = 0.02 mm for steel pipe piles. For concrete piles, δ_h can be taken equal to 0.04 (Ng.et al., 1988). The small strain shear modulus of sand can be estimated using the proposed correlation by Lo Presti (1987):

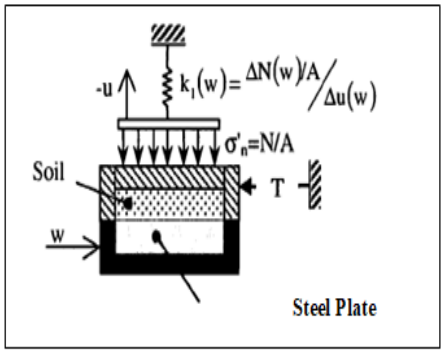

Figure 1**:** Direct shear test to simulate pile-soil interface skin friction (Fioravante, 2002)

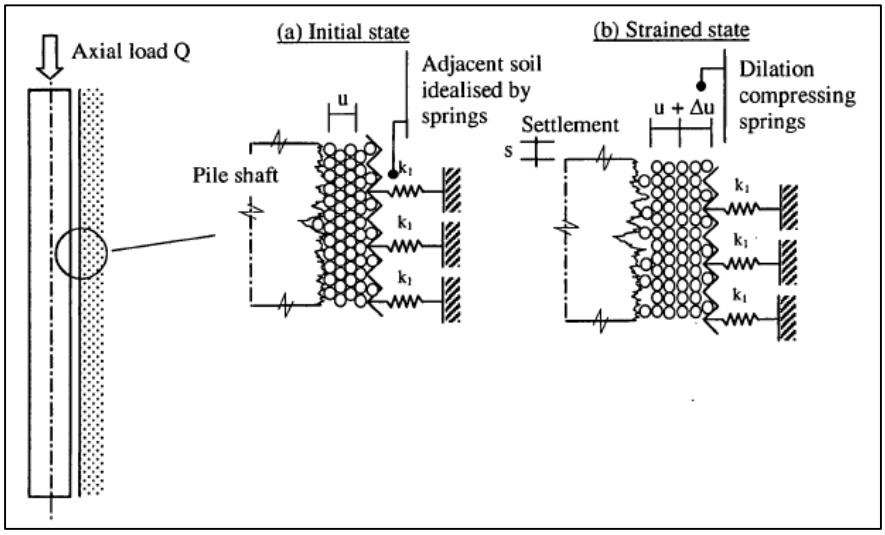

Figure 2: Soil-pile interface behavior (Fioravante, 2002)

ISSN:2788-6204

Table 3: Contribution of sand dilation to the measured shaft capacity (closed-ended piles)

Site No.	Serial No.	Pile No.	δ_f (°)	$\Delta\sigma'_{rd}$ (kN/m^2)	ΔK_d	$(\Delta\tau)_d$ (kN/m^2)	ΔQ_{sd} (kN)	$\boldsymbol{Q_{sc}}$ (kN)	$(\Delta Q_{sd}/Q_s)$ (%)
1	1	2	26	6.39	0.08	3.12	107.3	1572.7	6.4
	2	4	26	7.68	0.09	3.75	109.0	1671.0	6.1
	3	5	23	6.23	0.11	2.64	52.3	662.7	7.3
	4	6	26	6.51	0.08	3.18	100.9	1554.1	6.1
2	5	G-2	26	21.71	0.25	10.59	151.8	651.2	18.9
	6	B-5	26	14.85	0.21	7.24	137.0	868.0	13.6
3	7	G-7	30**	19.80	0.26	11.43	138.2	294.8	31.9
4	8	1	26	9.46	0.11	4.61	89.0	739.0	10.7
	9	2	26	7.02	0.08	3.42	88.1	911.9	8.8
	10	3	26	6.42	0.08	3.13	88.9	991.1	8.2
	11	4	26	**14.30**	0.23	7.00	110.7	709.3	13.5
	12	10	26	7.04	0.08	3.44	89.1	890.9	9.1
5	13	1	28	14.18	0.21	7.54	126.1	1001.9	11.2
	14	2	28	15.91	0.19	8.46	167.7	1132.3	12.9
	15	3	28	17.20	0.18	9.16	217.3	898.7	19.5
	16	4	28	15.91	0.19	8.46	167.7	955.3	14.9
6	17	H16	27	8.26	0.09	4.21	91.2	1448.8	5.9
7	18	A	26	3.73*	0..08	1.82	12.8	81.2	13.6
	19	D/A	26	5.20*	0.06	2.54	37.3	216.7	14.7
	20	E	26	6.20*	0.05	3.02	62.4	224.7	21.7
8	21	II	29	9.06	0.09	4.42	33.7	1072.3	3.0
9	22	TP2	29	21.69	0.17	12.02	22.5	27.5	45.0
10	23	5	26	7.40	0.56	3.61	237.1	2262.9	9.5

*For this site (very loose sand) S is taken 100,**Timber pile, δ_f is taken equal to φ_{cv}.

$$\frac{G_\circ}{P_a} = S\exp(cD_r)\left(\frac{\sigma'_c}{p_a}\right)^n \qquad (2-b)$$

Where S = modulus number that varies with silt content, c = parameter for the exponential variation of shear modulus with relative density, n = exponent in shear modulus variation with mean effective stress, σ'_c = average effective confining pressure calculated from:

$$\sigma'_c = \frac{(1+2K_\circ)}{3}\sigma'_{v,avg} \qquad (2-c)$$

Where $\sigma'_{v,avg}$ is the average effective vertical stress along the embedded depth of the pile and $K_\circ$ is the at-rest lateral earth pressure coefficient and for uncemented sand $K_\circ = (1-\sin\varphi)$. Randolph et al. (1994) suggested the use

ISSN:2788-6204

of $S = 400$, $c = 0.7$ and $n = 0.5$ for silica sand with S values being reduced for more compressible materials. Substitute Eq. (2b) in Eq. (2a) to get the following expression for $\Delta\sigma'_{rd}$ for steel pipe piles in silica sand:

$$\Delta\sigma'_{rd} = 3.2 \exp(0.70\, D_r) \left(\frac{1}{D}\right) \left(\frac{\sigma'_c}{P_a}\right)^{0.50} \qquad (2-d)$$

Table 4: Contribution of sand dilation to the measured shaft capacity (open-ended piles)

Site No.	Serial No.	Pile No.	δ_f (°)	$\Delta\sigma'_{rd}$ (kN/m^2)	ΔK_d	$(\Delta\tau)_d$ (kN/m^2)	ΔQ_{sd} (kN)	Q_{sc} (kN)	$(\Delta Q_{sd}/Q_s)$ (%)
8	1	I	29	9.14	0.17	5.07	40.1	776.9	4.9
	2	III	29	8.08	0.19	4.48	26.6	511.4	5.0
11	3	A	26	8.35	0.08	4.07	96.7	384.3	20.1
12	4	IA	26	1.80*	0.01	0.88	76.4	1560.6	4.7
13	5	P16	26	7.57	0.05	3.69	215.7	2315.3	8.5
14	6	322	26	13.87	0.15	6.76	129.4	572.6	18.4
16	7	1	29	6.97	0.07	3.86	155.5	1667.5	8.5
	8	2	29	6.97	0.07	3.86	155.5	1521.5	9.3
17	9	CS	26	10.12	0.14	4.94	57.6	330.4	14.9
18	10	1	26	7.56	0.08	3.69	189.6	2310.4	7.8
19	11	R1	29	9.20	0.09	5.10	148.4	1301.6	10.2
20	12	Ia	29.	7.13	0.05	3.95	287.7	2712.3	9.6
	13	Ib	29	8.35	0.04	4.63	427.4	9322.6	4.4
	14	II	29	9.09	0.04	6.17	561.5	10438.5	5.1

*For this site (loose sand) S is taken 100.

The increase in the magnitude of radial effective stress during loading for concrete piles is higher than that for steel piles because of differences in pile surface roughness and interface dilation. An interface boundary displacement (δ_h) of 0.02 mm for steel piles and 0.04 mm for concrete piles were used in this study. The value of δ_h of 0.04 mm for concrete piles was chosen, because it corresponds well to the data of loading tests on instrumented concrete piles carried out by Ng et al. (1988). Eq. (2a) showed good correlation with measured increases in horizontal (radial) stresses from a database by Chow (1997) of mainly small-scale tests on instrumented steel piles when δ_h was taken 0.02mm. As such, for concrete piles, the calculated $\Delta\sigma'_{rd}$ value from Eq. (2d) should be multiplied by 2. The radial effective stress increase during axial loading, $\Delta\sigma'_{rd}$, for each pile in the database is calculated and the results are summarized in Tables (3) and (4) for the closed and open-ended piles, respectively. The calculated $\Delta\sigma'_{rd}$ value for each pile is multiplied by $tan\delta_f$ to get $(\Delta\tau_f)_d$. The contribution of sand dilation to the measured shaft capacity ΔQ_{sd} is then calculated by multiplying $(\Delta\tau_f)_d$ by the pile surface area $A_s (A_s = \pi\, D\, L)$. The interface friction angle, δ_f, is taken 4° less than the constant volume friction angle of sand, φ_{cv} (Randolph et al., 1994; Lehane et al., 1993). The calculated

ISSN:2788-6204

$(\Delta\tau_f)_d$ and (ΔQ_{sd}) are also summarized in Tables (3) and (4) for the closed and open-ended piles, respectively. Also, summarized in Tables (3) and (4) the increase in the magnitude of average lateral earth pressure coefficient due to the tendency of the sand to dilate during pile axial loading (ΔK_d) which is calculated from:

$$\Delta K_d = \frac{\Delta\sigma'_{rd}}{\sigma'_{v,avg}} \qquad (2-\text{e})$$

From the calculated ratio$(\Delta Q_{sd}/Q_s)$ in Tables (3) and (4), it can be concluded that:

- The contribution of sand dilation to the measured shaft capacity is significant for driven piles with diameter less than 0.40 m especially in medium dense and dense sand at relatively low stress level. In Table (4) pile TP-2 at site (9) is a short pile with penetration depth of 5.95m and diameter of 0.1m driven in medium-dense sand with $D_r = 45\%$. The calculated ΔQ_{sd} was about 45% of the measured shaft capacity. Also pile G-7 at site (3) is a short pile with penetration depth of 11.67 m and diameter of 0.33 m driven in sand with $D_r = 55\%$. The calculated ratio for this pile $(\Delta Q_{sd}/Q_s)$ was about 32%.

- The analysis showed that the contribution of sand dilation during pile axial loading to the measured shaft capacity is likely to be insignificant for piles with diameters greater than 0.60 m especially at relatively high average stress level (greater than 150 kPa), the ratio $(\Delta Q_{sd}/Q_s)$ is generally less than 10%.

- Driven piles with small diameter (less than 0.4m) in loose sand and at relatively low stress level, showed some contribution of sand dilation to the measured shaft capacity.

- This indicates that test results of small diameter piles (laboratory piles) can't be directly extrapolated to prototype piles in the field due to significant sand dilation during model pile axial loading.

- The increase in radial effective stress during axial loading of small diameter piles in medium dense and dense sand encourage the use of micro-piles (diameter between 10 and 25 cm installed in a predrilled hole and surrounded by compacted sand) as a technique to reduce heave of footings constructed over highly expansive clay.

2.2 Contribution of Stationary Radial Effective Stresses to Shaft Capacity (Q_{sc}) for the Closed-Ended Piles.

2.2.1 Closed-Ended Piles

Contribution of stationary radial effective stresses to shaft friction capacity (Q_{sc}), can be calculated from Eq. (1-f). The stationary effective radial stress, σ'_{rc}, can be written as:

$$\sigma'_{rc} = K_c(z)\sigma'_v(z) \qquad (3)$$

Where K_c= stationary lateral earth pressure coefficient at depth (z) after pile driving and before loading and $\sigma'_v(z)$ = vertical effective stress at depth (z). During pile driving and for a given soil horizon, the sand adjacent to the pile surface is subjected to cyclic shear stress reversal with full magnitude which tends to degrade the local unit shaft friction (i.e. lateral earth pressure coefficient) as the pile tip penetrates down. This process is termed "friction fatigue" (Toolan et al. 1990, Randolph et al., 1994; Alawneh, 1999). To model the friction fatigue processes during pile driving, the following expression for $K_c(z)$ is used (Alawneh, 1999):

$$K_c(z) = K_{min} + (K_{max} - K_{min})\, exp\left(-\mu\left(\frac{L-z}{D}\right)\right) \qquad (4-a)$$

Where K_{max} maximum lateral earth pressure coefficient (at the pile tip) and μ is the rate of the exponential decay. Theoretically the minimum earth pressure coefficient, K_{min} can be taken equal to Rankine's active earth pressure coefficient (K_a) but Alawneh (1999) proposed the use of K_{min} as 0.23 which was the minimum average back-calculated value of lateral earth pressure coefficient for the database used in his study. Alawneh (1999) found that K_{max} for closed-ended piles, which is upper bounded by Rankine's passive earth pressure coefficient (K_p), increases

ISSN:2788-6204

exponentially with sand relative density (D_r) and decreases with increase in vertical effective stress at the pile tip ($\sigma'_{v,tip}$). Based on this, a rational expression for $K_{\max}$ to use in Eq. (4a) (for the stationary case before pile loading) is:

$$K_{max} = a.exp(bD_r)\left(\frac{\sigma'_{v,tip}}{P_a}\right)^c \qquad (4-b)$$

Where a, b, and c are statistical constants that need to be determined based on field data. For the exponential decay rate, μ, Alawneh (1999) proposed a value of 0.03. Randolph et al. (1994) pointed out that a more reasonable value of μ is 0.05 and stated that there is an indication that the value of μ tends to decrease with increasing pile diameter. Alawneh et al. (2019) found that it is more appropriate to relate μ to pile diameter using the following equation:

$$\mu = -0.1\ \log_{10} D \qquad for\ D \le 1\,m, \qquad 0.0 \le \mu \le 0.05 \qquad (5)$$

For $D > 1$ m, use $\mu = 0.0$

2.2.2 Correlation for K_{max} at the Pile Tip (Closed-Ended Pils)

The measured shaft friction capacity for each closed-ended pile in the database is divided in two components; ΔQ_{sd} and Q_{sc} as it was presented earlier. The stationary value, Q_{sc}, is calculated by subtracting the dilation component, ΔQ_{sd}, from the measured shaft friction capacity, $(Q_s)_{measured}$. The calculated Q_{sc} value for each pile in the database is summarized in Table (5). The calculated Q_{sc} value is then used to back-calculated the lateral earth pressure coefficient at the pile tip (K_{max}) as follows:

$$Q_{sc} = \pi\ D \int_0^L K_c(\gamma'_{avg}\ z)\ tan\delta_f\ dz \qquad (6-a)$$

Substitute Eq. (4a) into Eq. (6a), and perform the integration to get:

$$Q_{sc} = \pi\ D\ \gamma'_{avg}\ tan\delta_f \left[K_{min}\frac{L^2}{2} + (K_{max} - K_{min})\left[\frac{L\ D}{\mu} - \frac{D^2}{\mu^2} + \frac{D^2}{\mu^2}e^{-\frac{\mu L}{D}}\right]\right] \qquad (6-b)$$

The back-calculated (K_{max}) from Eq. (6b) is:

$$K_{max} = \frac{(Q_{sc}/(\pi\ D\ \gamma'_{avg}\ tan\delta_f)) - (K_{min}\ L^2/2)}{\frac{L\ D}{\mu} - \frac{D^2}{\mu^2} + \frac{D^2}{\mu^2}e^{-\frac{\mu L}{D}}} + K_{min} \qquad (6-c)$$

The back-calculated K_{max} values from Eq. (6c) which are summarized in Table (5) are correlated to sand relative density and vertical effective stress at the pile tip using the statistical package SPSS through the following relationship:

$$K_{max} = (K_{tip})_{CE} = 0.322\exp(0.028\ D_r)\left(\frac{\sigma'_{v,tip}}{P_a}\right)^{-0.84} \qquad (7)$$

2.2.3 Correlation for K_{max} at the Pile Tip (Open-Ended Pile)

For an open-ended pile driven in sand, the shaft friction capacity is generally lower than that for a similar closed-ended pile. The difference in shaft capacity between open and closed-ended piles depends on the penetration mode of the open-ended pile whether it is partially plugged, fully plugged or coring mode. Fully plugged pile experiences shaft capacity greater than that for a similar partially plugged pile. However, the difference in shaft friction capacity between open and closed-ended piles is significant along the lower part of the pile which is in the range of 8 times the pile diameter (Igoe et al., 2011). Along the upper part of the pile, it seems that there is no significant difference between unit shaft friction along open and closed-ended piles. To get the variation of unit shaft friction along an open-ended pile, Al Sharo et al. (2022) suggested multiplying the profile of unit shaft friction along a similar

ISSN:2788-6204

closed-ended pile by a correction factor, CF, which varies linearly along the pile from a maximum value of unity at the pile head to a minimum value of (M) at the pile tip:

$$\tau_{OE} = CF \times \tau_{CE} \quad (8-a)$$

$$CF = 1 - \left(\frac{1-M}{L}\right) z \quad (8-b)$$

$$M = (1.4\,\overline{FFR} - 0.11)\left(\frac{\sigma'_{v,tip}}{P_a}\right) \quad (8-c)$$

$$\overline{FFR} = 1 - FFR \quad (8-d)$$

Where τ_{OE}= unit shaft friction at any depth (z) of open-ended pile, τ_{CE}= unit shaft friction at any depth (z) of similar closed-ended pile, CF = correction factor which varies with depth and M = plug indicator which has a maximum value of unity and a minimum value of 0.12. So, very long open-ended pile with high $\sigma'_{v,tip}$ may experience the same shaft friction capacity for a similar closed-ended pile. Alternatively, the stationary shaft friction capacity of an open-ended pile can be calculated using the same approach for the closed-ended pile if the maximum lateral earth pressure coefficient at the tip of the open-ended pile is calculated from the following equation (Alawneh et al., 2019):

$$K_{max} = \left(K_{tip}\right)_{OE} = \left(K_{tip}\right)_{CE} M^n \quad (9-a)$$

$$n = 0.018\left(L/D\right) \quad (9-b)$$

Where $\left(K_{tip}\right)_{OE}$= lateral earth pressure coefficient at the tip of open-ended pile or $(K_{max})_{OE}$ and $\left(K_{tip}\right)_{CE}$= lateral earth pressure coefficient at the tip of a similar closed-ended pile or $(K_{max})_{CE}$.

In the field if the FFR is not measured then the FFR can be estimated from the plug length ratio, PLR (i.e. average incremental filling ratio, IFR_{avg}), using the correlation by Paik et al. (2003):

$$FFR = 1.09PLR - 0.22 \quad (9-c)$$

For driven piles in dense and very dense sand the average incremental filling ratio IFR_{avg} (i.e. the plug length ratio) can be estimated from the inner pile diameter (D_i) using the following equation (Lehane et al., 2005):

$$IFR_{avg} = PLR = \min.\left[\left(\frac{D_i\ in\ meters}{1.5}\right)^{0.2}, 1\right] \quad (9-d)$$

The lateral earth pressure coefficient at the tip of each open-ended pile in the database is calculated by substituting Eq. (7) into Eq. (9.a) to get:

$$\left(\mathrm{K_{tip}}\right)_{\mathrm{OE}} = \left(K_{max}\right)_{OE} = \left[0.322\exp(0.028\,\mathrm{D_r})\left(\frac{\sigma'_{\mathrm{v,tip}}}{\mathrm{P_a}}\right)^{-0.84}\right][\mathrm{M}]^{\mathrm{n}} \quad (10)$$

Eq. (10) together with Eq. (6b) is used to calculate the shaft capacity which comes from the stationary radial effective stress for each open-ended pile in the database and the results are summarized in Table (6). Also, summarized in Table (6) the calculated contribution of sand dilation to shaft friction capacity and the ratio of calculated to measured shaft capacity. The ratio of calculated to measured shaft capacity varies from 0.58 to 1.50 with average value of 1.01 and standard deviation of 0.29 indicating that the proposed methodology yields reasonable predictions. Figure (3) shows a plot of calculated versus measured shaft capacity of the open-ended piles.

ISSN:2788-6204

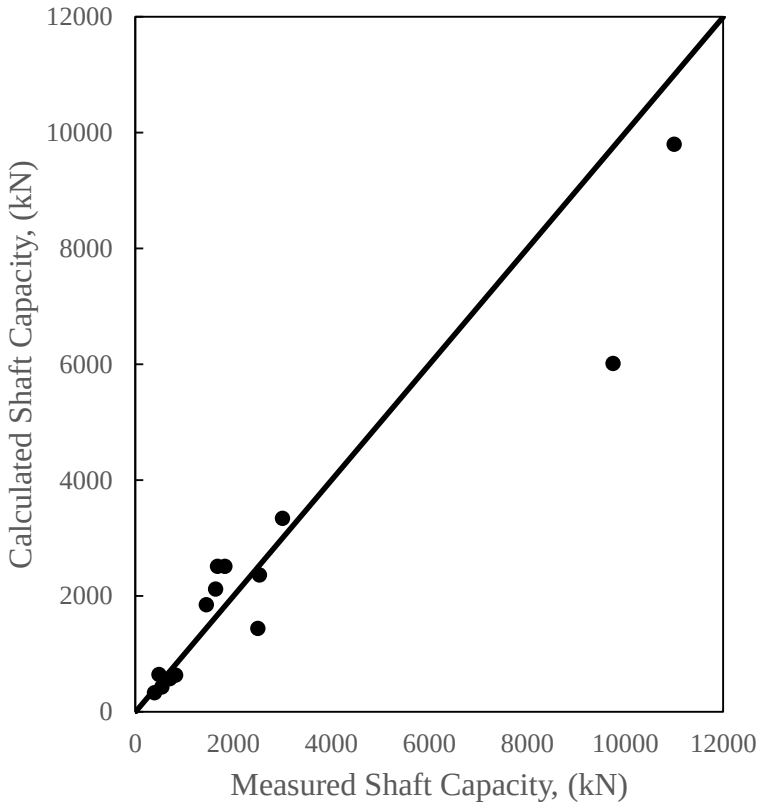

Figure 2: Calculated versus measured shaft capacity of the open-ended piles

2.3 Proposed Design Method

On the basis of the work presented in this study, a method is proposed for estimating the ultimate shaft friction capacity of a driven pile in sand. The main steps in the proposed method are:

(1) Estimate the average relative density and average effective unit weight of sand over the full length of the pile.

(2) Determine the magnitude of $K_{max} = \left(K_{tip}\right)_{CE}$ at the pile tip following Eq. (7) for closed-ended piles. For open-ended piles determine $K_{max} = \left(K_{tip}\right)_{CE} M^n$ where M is calculated from Eq. (8c).

(3) Evaluate the average value of the stationary lateral earth pressure coefficient $(K_c)_{ave.}$ as follows:

$$(K_c)_{ave.} = \frac{1}{L}\int_0^L K(z)\,.\,dz \qquad (11-a)$$

$$(K_c)_{ave.} = \frac{1}{L}\left[K_{min}L + \frac{D}{\mu}(K_{max} - K_{min})(1 - e^{-\frac{\mu L}{D}})\right] \qquad (11-b)$$

(4) Evaluate the increase in radial effective stress due to sand dilation $\Delta\sigma'_{rd}$ using Eq. (2d) for steel piles, for concrete piles multiply the calculated $\Delta\sigma'_{rd}$ value from Eq. (2d) by 2. The increase in lateral earth pressure due to sand dilation ΔK_d can be obtained by dividing $\Delta\sigma'_{rd}$ by the average vertical effective stress $\sigma'_{v,avg}$.

(5) Find the average lateral earth pressure coefficient at failure K_{avg} as the sum of ΔK_d and. $(K_c)_{ave.}$

(6) Evaluate the average unit shaft resistance at ultimate uplift loading using the following equation:

ISSN:2788-6204

$$(\tau_f)_{avg} = \left(K_{avg}\sigma'_{v,avg}\right)\tan(\delta_f) \qquad (11-c)$$

(7) Estimate the ultimate uplift shaft friction capacity by multiplying $(\tau_f)_{avg}$ by the pile surface area.

$$Q_s = (\tau_f)_{avg}.A_s \qquad (11-d)$$

(8) The shaft friction capacity in compression loading can be obtained by multiplying the shaft resistance in tension by 1.25 according to API RP 2GEO (2014).

Table 5: Back-calculated K_{max} for the closed-ended piles.

Site No.	Serial No.	Pile No.	Q_{sc} (kN)	The back-calculated K_{max}
1	1	2	1572.7	1.45
	2	4	1671.0	2.11
	3	5	662.7	1.90
	4	6	1554.1	1.70
2	5	G-2	651.2	1.32
	6	B-5	868.0	1.37
3	7	G-7	294.8	0.75
4	8	1	739.0	1.42
	9	2	911.9	1.09
	10	3	991.1	1.02
	11	4	709.3	1.97
	12	10	890.9	1.05
5	13	1	1001.9	1.98
	14	2	1132.3	1.70
	15	3	898.7	0.97
	16	4	955.3	1.42
6	17	H-16	1448.8	1.97
7	18	A	81.2	0.68
	19	D/A	216.7	0.50
	20	E	224.7	0.23
8	21	II	1072.3	5.00
9	22	TP2	27.5	1.21
10	23	5	2262.9	0.55

ISSN:2788-6204

Table 6: Prediction of shaft capacity of open-ended piles.

Serial No.	Pile No.	PLR	FFR*	[M]	n	$(K_{tip})_{CE}$	$(K_{tip})_{OE}$	Calc. Q_{sc} (kN)	Calc. ΔQ_{sd} (kN)	Calc. Q_{sc} (kN)	Meas. Q_s (kN)	$\frac{(Q_s)_{calc.}}{(Q_s)_{meas.}}$
1	I	0.66+	0.50	0.65	0.35	3.69	3.18	598.6	40.2	638.8	817	0.78
2	III	0.77+	0.62	0.36	0.26	4.54	3.48	407.2	26.6	433.8	538	0.81
3	A	0.87+	0.73	0.42	0.52	1.16	0.73	553.5	96.7	650.2	481	1.35
4	IA	0.84++	0.70	1.0	1.00	0.29	0.29	2046.2	76.3	2122.5	1637	1.30
5	P16	0.84++	0.70	0.89	0.90	0.71	0.64	2149.5	215.7	2365.2	2531	0.93
6	322	0.71++	0.55	0.99	1.00	0.97	0.97	446.3	129.4	575.7	702	0.82
7	1	0.84++	0.7	0.59	0.62	1.86	1.34	2359.9	155.5	2515.4	1823	1.38
8	2	0.84++	0.70	0.59	0.62	1.86	1.34	2359.9	155.5	2515.4	1677	1.50
9	CS	0.73++	0.58	0.67	0.65	1.29	1.00	276.5	57.6	334.1	388	0.86
10	1	0.91++	0.77	0.38	0.36	0.80	0.57	1256.1	189.6	1445.7	2500	0.58
11	R1	0.78+	0.63	0.86	0.72	1.53	1.37	1703.8	148.4	1852.2	1450	1.28
12	Ia	0.99+	0.86	0.28	0.72	1.31	0.52	3064.4	287.7	3343.1	3000	1.11
13	Ib	0.97+	0.84	0.46	0.91	1.24	0.61	5587.8	427.4	6015.5	9750	0.62
14	II	0.95+	0.82	0.68	1.00	1.08	0.73	9230.2	561.5	9801.7	11000	0.89

+measured value, ++calculated from Eq. (9d), *calculated from Eq. (9c).

2.4 Example

Paik et al. (2003) reported results of static compression test conducted on full-scale closed-ended steel pipe pile with outside diameter of 0.356 m. The pile was driven to a depth of 6.85m at the Pigeon River sit, Indian. The soil profile consisted of 3.0 m loose sand (D_r = 30%) underlain by a dense gravelly sand layer (D_r = 80%). Estimated friction angle was 30° and 40° for the loose and dense sand, respectively. Two meters of fill was removed from the site before pile installation and the ground water table was at 3.0 m below ground surface after fill removal. As reported by Paik et al. (2003), pile-sand friction angle = 22.2°, effective unit weight of soil above GWT = 17 kN/m^3, effective unit weight of soil below GWT = 11 kN/m^3. The reported measured shaft capacity in compression for this pile was 425 kN.

2.4.1 Prediction of pile capacity:

Vertical effective stress at the pile tip = 93.3 kN/m^2, K_{min} = 0.23, and μ = 0.045, average effective vertical stress for the loose sand layer = 25.5 kN/m^2, average effective vertical stress for the dense sand layer = 72.2 kN/m^2.

Due to fill removal, the estimated average OCR for the loose sand layer = (2 x17+25.5)/25.5 = 2.33, K_o = (1-sin30°)(2.33)$^{0.5}$ = 0.76 and average effective confining pressure σ_c' = 21.42 kN/m^2.

Due to fill removal, the estimated average OCR for dense sand layer = (2 x17+72.2)/72.2 = 1.47 and K_o = (1-sin40°)(1.47)$^{0.5}$ = 0.43 and average effective confining pressure σ_c' = 44.76 kN/m^2.

ISSN:2788-6204

Loose sand: From Eqs. (2a, b), using D_r = 30%, S = 100, σ_c' = 21.42, the calculated $\Delta\sigma_{rd}'$ = 1.28 kN/m^2 and ΔK_d= 0.05

From Eq. (7) using D_r = 30%, K_{min} = 0.23, $\sigma_{v,tip}'$ = 93.3 kN/m^2, the calculated K_{max}= 0.79 , $(K_{max} - K_{min})$ = 0.56, μ = 0.045, the calculated $(K_c)_{ave.}$ = 0.516 and K_{avg} = 0.05 + 0.516 = 0.566. The calculated shaft capacity in loose sand $(Q_s)_{loose}$ is:

$(Q_s)_{loose}$= (0.566)(25.5)tan(22.2°)(3.14)(0.356)(3.0) = 19.8 kN.

Dense sand: From Eq. (2-d), using D_r = 80%, S = 400, σ_c' = 44.76 kN/m^2, the calculated $\Delta\sigma_{rd}'$ =10.53 kN/m^2 and ΔK_d= 0.15.

From Eq. (7) using D_r = 80%, K_{min} = 0.23, $\sigma_{v,tip}'$ = 93.3 kN/m^2, the calculated K_{max}= 3.21 , $(K_{max} - K_{min})$ = 2.98, μ = 0.045 the calculated $(K_c)_{ave.}$ = 2.55. and K_{avg} = 0.15 + 2.55 = 2.70. The calculated shaft capacity in dense sand $(Q_s)_{dense}$ is:

$(Q_s)_{dense}$= (2.7)(72.2)tan(22.2°)(3.14)(0.356)(3.85) = 342.4 kN.

So, for compression loading Q_s = 1.25(19.8+342.4) = 452.8 kN. The ratio of calculated to measured shaft capacity = 452.8/425 = 1.07 (good prediction).

3. Conclusions

Based on the analysis and results obtained from this study, the following conclusions are drawn:

(1) Changes in lateral earth pressure acting on the pile-sand interface occurs not only during pile driving but also during pile axial loading due to the tendency of the sand close to the pile surface to dilate during loading.

(2) The most important factors that affect the increase in shaft capacity due to sand dilation during loading are sand relative density, pile diameter and average effective vertical stress. The increase in the magnitude of lateral earth pressure coefficient during pile axial loading increase with increasing sand relative density and decreases with increase in pile diameter and average effective vertical stress.

(3) The contribution of sand dilation to pile shaft capacity is significant for piles with outside diameter less than 0.40 m especially if they are driven in medium dense to dense sand. For piles with outside diameters greater than 0.60 m, the contribution of sand dilation to pile shaft capacity is small (less than 10%) especially at relatively high stress level (greater than 150 kPa).

(4) The practical conclusion which can be drawn from this study is that results and findings derived from laboratory tests conducted on small-scale model piles in sand can't be extrapolated directly to piles in the field due to significant sand dilation in the laboratory tests which contributes to the measured model pile capacity (small pile diameter and low stress level).

(5) One important conclusion which can be drawn from this study is that direct shear test at a prescribed normal stiffness is the best to describe the interface behavior during axial loading of piles. In this test, the normal stress continuous to change due to the tendency of the sand to dilate during shear loading.

(6) New correlation was developed for the stationary lateral earth pressure coefficient before loading. This correlation together with Eq. (2-d) is used to propose a methodology to estimate shaft capacity of driven piles in sand. Prediction of shaft capacity of a well-documented field case showed good agreement with the measured shaft capacity indicating that the proposed approach is useful and can be used to predict shaft capacity of driven piles in sand.

Acknowledgments: Part of this research was supported by the ADDOPTML (ADDitively Manufactured OPTimized Structures by means of Machine Learning) project (NO: 101007595) belonging to the Marie Sklodowska-Curie Actions (MSCA) Research and Innovation Staff Exchange (RISE) H2020-MSCA-RISE-2020. Their support is highly acknowledged. The authors would also like to thank the Jordan university of Science and Technology for its support.

ISSN:2788-6204

LIST OF ABBREVIATIONS

Abbreviation	Description
c	Parameter for the exponential variation of shear modulus with relative density
CF	Correction factor
D	Pile diameter
D_i	Inner diameter of open-ended pile
D_r	Sand relative density
FFR	The final filling ratio along the lower part of pile shaft
$\overline{FFR}$	The average final filling ratio
$G_\circ$	Small strain (initial tangent) shear modulus
IFR	Incremental filling ratio
IFR_{avg}	Average incremental filling ratio
K	Lateral earth pressure coefficient
K_a	Rankine's active earth pressure coefficient
K_c	Stationary lateral earth pressure coefficient after pile driving and before loading
K_{max}	Maximum value of earth pressure coefficient
K_{min}	Minimum value of earth pressure coefficient
K_o	At-rest earth pressure coefficient
K_p	Rankine's passive earth pressure coefficient
$(K_{tip})_{CE}$	Lateral earth pressure coefficient at the tip of a similar closed-ended pile
$(K_{tip})_{OE}$	Lateral earth pressure coefficient at the tip of open-ended pile
L	Pile penetration depth
M	Plug indicator
n	Exponent in shear modulus variation with mean effective stress
P_a	Atmospheric pressure (100 kpa)
PLR	Plug length ratio
Q_s	Shaft capacity of pile
Q_{sc}	Contribution of stationary radial stress to pile shaft capacity
$(Q_s)_{calculated}$	Calculated shaft capacity
$(Q_s)_{measured}$	Measured shaft capacity
S	Modulus number that varies with silt content
z	Depth below ground surface
γ'_{avg}	Average unit weight
ΔQ_{sd}	contribution of sand dilation to the measured shaft capacity
$(\Delta\tau)_d$	change in unit shaft friction during pile axial loading
ΔK_d	Change in lateral earth pressure coefficient during loading
$\Delta\sigma'_{rd}$	Chang in radial effective stress during pile axial loading
δ_f	Pile-soil friction angle at failure
δ_{cv}	Constant volume interface pile-soil friction angle
δ_h	Radial displacement of soil particles during pile driving
μ	The exponential decay coefficient of the lateral earth pressure coefficient

ISSN:2788-6204

Abbreviation	Description
σ_c'	Average effective confining pressure
σ_{rc}'	Radial stationary stress at the pile interface after pile installation
σ_{rf}'	Radial effective stress at failure
$\sigma_{v,avg}'$	Average effective vertical stress
$\sigma_{v,tip}'$	Vertical effective stress at the pile tip
$\sigma_v'(z)$	Vertical effective stress at depth z
τ_{CE}	Unit shaft friction at depth (z) for closed-ended pile
τ_{OE}	Unit shaft friction at depth (z) for open-ended pile
τ_f	Local unit shaft friction at failure
φ	Friction angle of sand
φ_{cv}	Constant volume friction angle of sand

References:

[1] Al Sharo, A., Alawneh, A., S. and Al Omari, E., M. (2022). Friction capacity of driven open-ended piles in sand. Arabian Journal of Geoscience.

[2] Alawneh, A. (1999). Tension piles in sand: A method including degradation of shaft friction during pile driving. Transportation Research Record, 1663(1), 41-49.

[3] Alawneh, A. S., Malkawi, A. I. H. & Al-Deeky, H. (1999). Tension tests on smooth and rough model piles in dry sand. Canadian geotechnical journal, 36(4), 746-753.

[4] Alawneh, A., Nusier, O. & Atiyeh, M. (2019). A New Approach for Estimating Capacity of Driven Piles in Sand under Tensile Loading. Jordan Journal of Civil Engineering, 13(3).

[5] American Petroleum Institute API Recommended Practice RP2GEO. (2014). Geotechnical and Foundation Design Considerations.1st Edition.

[6] Beringen, F. L., Windle, D., and Van Hooydonk, W. R. (1979). Results of loading tests on driven piles in sand. Recent Developments in the Design and Construction of Piles, Imperial College England, London.

[7] Brucy, F., Meunier, J. and Nauroy, J. F. (1991). Behavior of pile plug in sandy soils during and After driving. Proc., 23rd Annual Offshore Technology Conference, OTC 6514, Houston, Tex., pp. 145–154.

[8] Chow, F. C. (1997). Investigations into displacement pile behavior for offshore foundations. Ph. D Thesis, Univ. of London (Imperial College).C

[9] Chow, F.C., Jardine, R.,J., Brucy, F. and Nauroy, J.F.(1998). Effect of time on capacity of pipe piles in dense marine sand. J. of Geotech. And Geoenvir. Engng. ASCE. 124(3), pp. 254-264.

[10] Fioravante, V. (2002). On the shaft friction modelling of non-displacement piles in sand. Soils and foundations, 42(2), pp. 23-33.

[11] Furgo, B. V. (1969). Soil investigation, platform BD North Sea, Block 49/26. Report to Shell UK Expro., England.

ISSN:2788-6204

[12] Gregersen, O. S., Aas, G. and Dibagio, E. (1973). Load Tests on Friction Piles in Loose Sand. Proc., 8th International Conference on Soil Mechanics and Foundation Engineering, Moscow, Vol. 2, pp. 109–117.
[13] Igoe, D. J. P., Gavin, K. G. & O'Kelly, B. C. (2011). Shaft capacity of Open-Ended Piles in Sand. Journal of Geotechnical and Geoenvironmental Engineering, 137(10), 903-913.
[14] Jardine, R. J., Chow, F. C, Overy, R. F. and Standing J. R. (2005). ICP procedures for driven piles in sands and clays. Thomas Telford Limited, London.
[15] Jardine, R.J., Standing, J.R. (2000). Pile load testing performed for HSE cyclic loading study at Dunkirk, France Rep. No. OTO 2000007. Health and Safety Executive, London.
[16] Kollk, H.J., Baaijens, A.E. and Vergobi, P. (2005). Results of axial load tests on pipe piles in very dense sands, The Euripedes JIP. In, Proc. Int. Symp. On Frontiers in Offshore Geomechanics, ISFOG, Taylor and Francis, London, pp. 661-667.
[17] Lehane, B. & Jardine, R. J. (1994). Shaft capacity of driven piles in sand: a new design method. In 7th International Conference on the behaviour of offshore structures (pp. 23-26). Pergamon.
[18] Lehane, B. M., Jardine, R. J., Bond, A. J. and Frank. R. (1993). Mechanisms of shaft friction in sand from instrumented pile tests. Journal of Geotechnical Engineering, Vol. 119, No. 1, pp. 19–35.
[19] Lehane, B. M., Schnider, J. A. & Xu, X. (2005). Evaluation of design methods for displacement piles in sand. UWA Report, GEO, 5341.
[20] Lo Presti, D. (1987). Mechanical behaviour of Ticino sand from resonant column tests. Polytechnic University of Turin, Italy.
[21] Mansur, C. I., and Hunter, A. H. (1970). Pile tests—Arkansas River Project. Journal of the Soil Mechanics and Foundations Division, ASCE, Vol. 96, No. SM5, pp. 1545–1582.
[22] Mansur, C. I., Robert, I., and Kaufman, J. M. (1958). Piles tests, Low-Sill Structure, Old River, Louisiana. Transactions of the American Society of Civil Engineers, Vol. 123, No. 2936, pp. 715–743.
[23] McCammon, N. R. and Golder, H. Q. (1970). Some loading tests on long pipe piles. Geotechnique, Vol. 20, No. 2, pp. 171–184.
[24] McClelland Engineers, Inc. (1958). pullout tests, piles driven into sand. Padre Island, Tex., Report to Shell Oil Company, Texas.
[25] Mey, R., Oteo, C. S., Sanchez Del Rio, J. and Seriano, A. (1985). Field testing on large driven piles. Proc., 11th International Conference on Soil Mechanics, San Francisco, Calif., pp. 1559–1564.
[26] Ng, E. S., Tsang, S. K. & Auld, B. C. (1988). Pile foundation: the behavior of piles in cohesionless soils. Federal Highway Administration, Washington. DC Report FHWA-RD-88–081.
[27] Nottingham, L. C. (1975). Use of quasi-static friction cone penetrometer data to predict load capacity of displacement piles. Ph.D. thesis. University of Florida, pp. 1559–1564.
[28] Paik, K., Salgado, R., Lee, J. & Kim, B. (2003). Behavior of open-and closed-ended piles driven into sands. Journal of Geotechnical and Geoenvironmental Engineering, 129(4), 296-306.
[29] Randolph, M. F., Dolwin, R. & Beck, R. (1994). Design of driven piles in sand. Geotechnique, 44(3), 427-448.
[30] Reese, L. C., and Cox, W. R. (1976). Pullout tests of piles in sand. Proc., Offshore Technology Conference, Paper No. 2472.

ISSN:2788-6204

[31] Sherman, Jr. W. C., Holloway, D. M. and Trahan, C. C. (1974). Analysis of pile tests. Technical Report S-74-3, U.S. Army Engineer Waterways Experiment Station, Vicksburg, Miss. Tex. pp. 33–42.

[32] Toolan, F. E., Lings, M. L., Bristol, U., and Mirza, U. A. (1990). An appraisal of API RP2A recommendations for determining skin friction of piles in sand. Proc., 22nd Annual Offshore Technology Conference, Houston.

[33] Vesic, A. S. (1970). Tests on instrumented piles, Ogeechee River Site. Journal of the Soil Mechanics and Foundations Division, ASCE, Vol. 96, No. SM2, pp. 561–584.

[34] Yen, T. L., Lin, H. and Chin, C. T. (1989). Interpretation of instrumented driven steel pipe piles. Foundation Engineering: Current Principles and Practices, Vol. 2. American Society of Civil Engineers, New York, pp. 1293–1309.